

TECTONIC FEATURES IN WESTERN ARABIA TERRA AND THEIR IMPLICATIONS FOR THE EXOMARS 2022 ROVER LANDING SITE.

S. Z. Woodley*, P. Fawdon, M. R. Balme, D. A. Rothery, and E. Favaro. The Open University, Walton Hall, Milton Keynes, United Kingdom. *savana.woodley@open.ac.uk

Introduction: Oxia Planum, the landing site of the ExoMars Rosalind Franklin rover [1], is located in transitional terrain between the Arabia Terra highlands and the Chryse Planitia lowlands (Fig 1). Recent work shows that Arabia Terra hosted extensive river systems during the Noachian period (> 3.7 billion years ago) [2, 3]. In our study area in west Arabia Terra (Fig 1b), the fluvial landscape has been exhumed from beneath younger sedimentary terrains [e.g. 4] while also being modified by tectonism. The impact of tectonism, on both regional and global scales, on the geological history of west Arabia Terra is poorly understood; it could have implications for palaeohydrology and the elevation of proposed shoreline features. To provide constraints on the tectonic evolution of the region, we have constructed a preliminary map of tectonic features in west Arabia Terra (Fig 1) and analyzed their orientations.

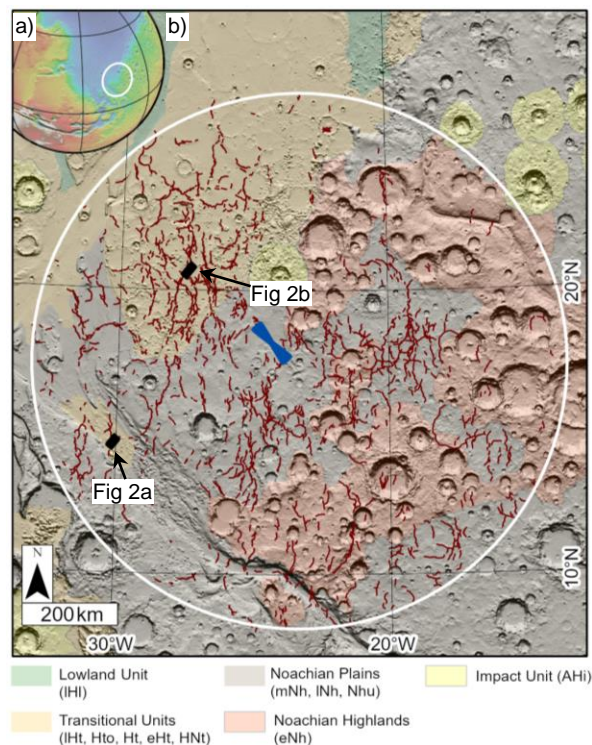


Figure 1. a) Global MOLA topographic map showing location of study area in west Arabia Terra. **b)** Map of tectonic features (red) in the study area (white circle), on a geological base map [12]. The landing “ellipse” of the ExoMars rover in Oxia Planum is shown in blue.

Our study site is a 1 million km² area centered on Kilkhampton crater in Oxia Planum (Fig 1b). Tectonic features occur across the region including near the ExoMars rover landing site and in the channel floors of Ares, Coogoon, and Mawrth Valles.

Wrinkle ridges are the most common tectonic structures in the study area; these are curvilinear topographic highs that are morphologically complex and varied [e.g. 5; Fig 2b]. Wrinkle ridges generally consist of a broad rise, a superposed ridge, and a small crenulation. These three elements are commonly described as first, second, and third order ridges respectively [6], but any one of these elements can be absent in an individual wrinkle ridge. The accepted interpretation of wrinkle ridges as tectonic features that formed by compressional faulting and folding [7] is based on observations of vertical offset across ridges, ridges traceable along their length into fault scarps (Fig 2b), offset of pre-existing craters, and comparison to terrestrial analogs [e.g. 6, 7].

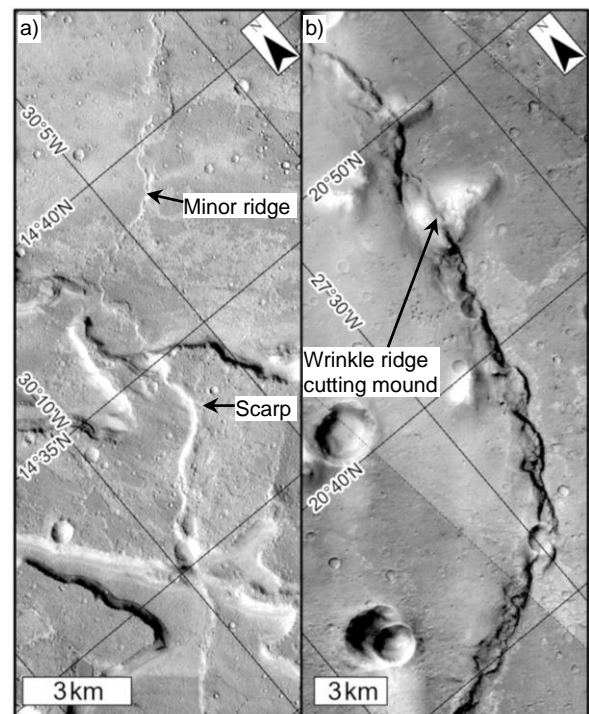


Figure 2. Example of various morphologies of tectonic features in study area. **a)** Minor wrinkle ridge and scarp-like ridge on the floor of Ares Vallis. **b)** Major wrinkle ridge in Chryse Planitia. (CTX images)

Methods: Fig 1b shows a preliminary map of tectonic features in the study area. The extent of the study area was chosen to include both highland and lowland terrain as well as the three previously mentioned Valles. At this stage of the study, we have only digitized the ‘crests’ of the tectonic features. We digitized features at a scale of 1:50,000 using 6 m/pixel Context Camera (CTX) images [8], 100 m/pixel Thermal Emission Imaging System (THEMIS) daytime infrared images [9], and 463 m/pixel gridded topographic data from the Mars Orbiter Laser Altimeter (MOLA) [10]. In order to account for illumination bias and to prevent east-west oriented ridges being overlooked, we also used High Resolution Stereo Camera (HRSC) [11] hillshades constructed using multiple sun angles.

To analyze the orientations of the tectonic features, we subdivided each ridge into 500 m long sections. For each 500 m section, we measured bidirectional orientations, omitting sections <500 m. The bidirectional orientations of the 500 m sections are shown in a rose diagram in Fig 3.

Observations: We have identified numerous wrinkle ridges in western Arabia Terra, with a combined length of ~20,000 km. Our map shows that tectonic features occur across the highland-lowland transition region and deform geomorphic units of all ages (Fig 1; [12]). However, the features appear to be predominantly concentrated in Noachian Plains units and Transition units. Fig 3 shows that the bidirectional orientation of wrinkle ridges is predominantly north-south trending; East-west trending wrinkle ridges are approximately a factor of three less common.

Interpretation: We suggest that the occurrence of tectonic features in units of all ages, coupled with the heterogenous distribution of features across units, indicates that multiple phases of tectonic activity occurred. This is in agreement with [3], who propose that there have been multiple episodes of tectonic and aqueous activity. We do not yet draw conclusions about the relationship between fluvial and tectonic features, as further study is required to determine their relative ages.

Our observations of predominantly north-south trending tectonic features in west Arabia Terra are broadly in line with expected trends of Tharsis-related tectonism in Mars’ western hemisphere [e.g. 13]. This shows that the small scale features similarly conform to the global tectonic stress regime. We have not yet explored the possible contribution of basin related stresses or stresses related to the dichotomy boundary.

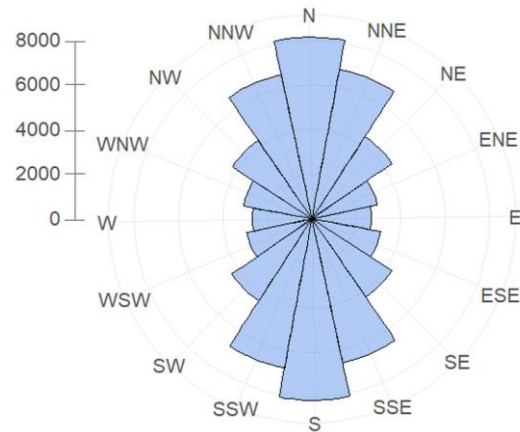


Figure 3. Rose diagram of the bidirectional orientations of 500 m long sections ($n = 78,036$) of the wrinkle ridge crests in the study area. Axes represents segment count for each orientation.

Conclusion: We present preliminary findings of a tectonic mapping survey in western Arabia Terra, performed CTX images. We suggest that multiple phases of tectonic activity were responsible for the widespread tectonic deformation. The predominantly north-south orientation of the tectonic features is in line with expected global trends.

Acknowledgments: We gratefully acknowledge funding from STFC grant ST/V50693X/1 and the Open University STEM Faculty (SZW), and UK Space Agency ST/R001413/1 (PF, MRB).

References: [1] Vago, J.L. et al. (2017) *Astrobiology*, 17, pp. 471-510. [2] Davis, J.M. et al. (2016) *Geol.*, 44, pp. 847-850. [3] Fawdon, P. et al. (2019) *LPSC abstract, LPI Contrib. No. 2132*. [4] Quantin-Nataf, C. et al. (2020; in press) *Astrobiology*. [5] Strom, R.G. (1972) *Mod. Geol.*, 2, 133-157. [6] Watters, T.R. (1988) *JGR: Solid Earth*, 93, 10236-10254. [7] Plescia, J.B. and Golombek, M.P. (1986) *Geol. Soc. Am. Bull.*, 97.11, 1289-1299. [8] Malin M.C. et al. (2007) *J Geophys Res*, 112,1-25. [9] Christensen, P.R., et al. (2004) *Space Sci. Rev.* 110, 85–130. [10] Smith, D. E., et al. (2001) *J. Geophys. Res.*, 106, 23689–23722. [11] Neukum, G. and Jaumann, R. (2004) *ESA Special Publication, 1240*, 17–35. [12] Tanaka K.L. et al. (2014) *USGS Scientific Investigations Map 3292*. [13] Watters, T. (1993) *J Geophys Res*, 98, 17049-17060.